

Characterization of exposure to silver nanoparticles in a manufacturing facility

Junsu Park · Byoung Kyu Kwak · Eunjoo Bae · Jeongjin Lee · Younghun Kim · Kyunghee Choi · Jongheop Yi

Received: 31 January 2009 / Accepted: 21 July 2009 / Published online: 2 August 2009
© Springer Science+Business Media B.V. 2009

Abstract An assessment of the extent of exposure to nanomaterials in the workplace will be helpful in improving the occupational safety of workers. It is essential that the exposure data in the workplace are concerned with risk management to evaluate and reduce worker exposure. In a manufacturing facility dealing with nanomaterials, some exposure data for gas-phase reactions are available, but much less information is available regarding liquid-phase reactions. Although the potential for inhaling nanomaterials in a liquid-phase process is less than that for gas-phase, the risks of exposure during wet-chemistry processes are not negligible. In this study, we monitored and analyzed the exposure characteristics of silver nanoparticles during a liquid-phase process in a commercial production facility. Based on the

measured exposure data, the source of Ag nanoparticles emitted during the production processes was identified and a mechanism for the growth of Ag nanoparticle released is proposed. The data reported in this study could be used to establish occupational safety guidelines in the nanotechnology workplace, especially in a liquid-phase production facility.

Keywords Exposure assessment · Field monitoring · Liquid-phase process · Silver nanoparticles · SMPS · Occupational safety · EHS

Introduction

Many countries are currently supporting research and development on the production of nanomaterials due to the considerable economic potential of nanotechnology and the fact that products containing nanomaterials are increasing very rapidly. It is predicted that nanotechnology will have a \$3.1 trillion impact on the global economy by 2015 (Schmidt 2009). However, numerous knowledge gaps are evident regarding the advantages and disadvantages associated with nanotechnology. Nanomaterials may have a significant impact on the environment and human health. Filling these knowledge gaps is essential to ensure the safe development of nanotechnology. International organizations, government agencies,

J. Park · B. K. Kwak · E. Bae · J. Lee · J. Yi (✉)
School of Chemical and Biological Engineering, Institute of Chemical Processes, Seoul National University, Shillim-dong, Kwanak-gu, Seoul 151-742, Korea
e-mail: jyi@snu.ac.kr

Y. Kim
Department of Chemical Engineering, Kwangwoon University, Wolgye-dong, Nowon-gu, Seoul 139-701, Korea

K. Choi
National Institute of Environmental Research, Incheon 404-170, Korea

academia and the private sector are currently attempting to fill these knowledge gaps.

The number of workers who deal with nanomaterials is expected to increase rapidly as the use of the nanomaterial increase in the future. Nanomaterials that are released in the workplace can be easily inhaled and deposited in lungs or other organs of the workers (Kreyling et al. 2002; Oberdörster et al. 1995). Many nanotechnology companies are attempting to minimize the extent of exposure to nanomaterials during production processes for worker protection (Helland et al. 2008). Therefore, a strategic effort to control exposure to nanomaterials in the workplace is currently underway, with international cooperation, from organizations such as the OECD working party on the manufactured nanomaterials steering group 8 (WPMN SG8). It is essential reliable exposure data in the workplace be obtained, to identify the pathways associated with exposure, the magnitude of exposure, and the frequency of potential exposure. To date, the majority of field studies on exposure have been conducted for the gas-phase production process because the release of nanoparticles from powders and the direct emission of aerosols into the air clearly represent major potential sources (Maynard and Kuempel 2005). Although the potential for inhaling a nanomaterial in a liquid-phase process is smaller than that for the gas or vapor-phase processes, risks associated with exposure to nanomaterials during a liquid-phase process should not be neglected, because many of the recently developed nanomaterials are produced via wet chemistry which include the sol–gel process for TiO₂ nanoparticles (Yun et al. 2008), Ag nanoparticles (Park and Kim 2008), and Fe₂O₃ nanoparticles (Park et al. 2005). However, there are few reports on exposure to aerosolized nanomaterials during the liquid-phase process.

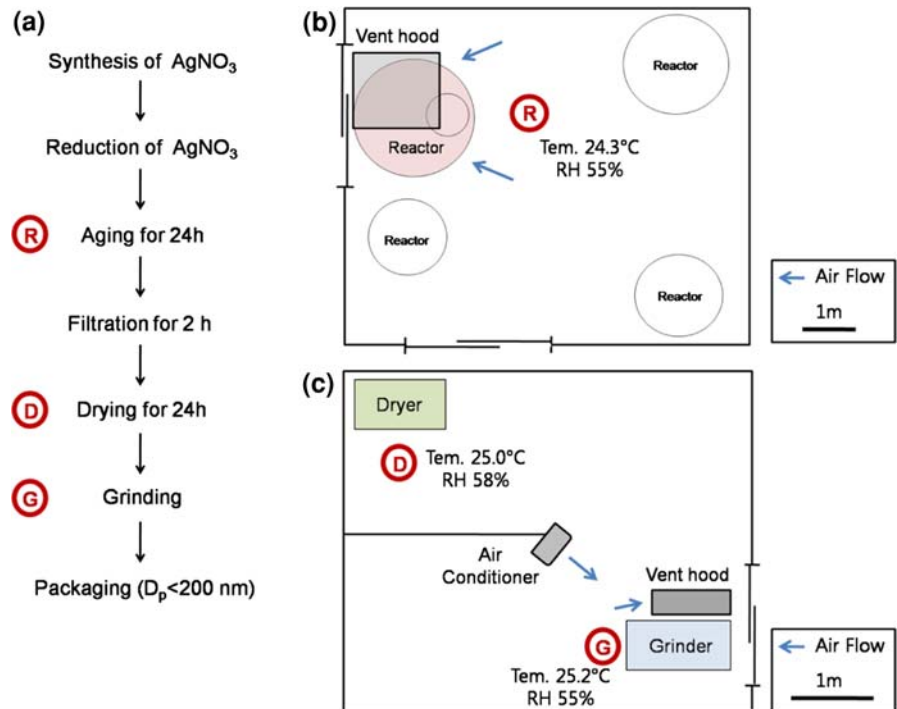
This study reports on field exposure measurements related to Ag nanoparticles during the liquid-phase production process at a commercial production facility in Korea. Based on the measured exposure data, the sources of emission of Ag nanoparticles during the production process were indentified, and the growth mechanism of Ag nanoparticles released into the atmosphere of the workplace is proposed. These data would be useful in terms of preparing occupational safety guidelines for a liquid-phase process.

Experimental

Monitoring locations

Exposure to Ag nanoparticles was measured at an Ag nanoparticle production facility in Korea. The facility produces approximately 3,000 kg of silver nanoparticles per month. This large scale production system is suitable for the identification of emission sources during liquid-phase production process. The stages for the production of Ag nanoparticles can largely be divided into four steps, namely: a batch reaction process based on wet chemical methods, followed by filtering, drying, and grinding, as shown in Fig. 1a. In this process, bulky silver was synthesized by the liquid-phase reaction of silver nitrate (AgNO₃) with nitric acid. Acidic gases generated as the result of the preparation of AgNO₃ were trapped and removed by an acidic gas removal system which was directly connected to the reactor. A colloidal suspension of silver was produced by the reduction of AgNO₃ in the presence of a dispersing agent. The reactor room is located on the second floor which is 3 m higher than the first floor. Monitoring in the reaction room was performed at site ‘R’ which was located at a distance of 1 m from the reactor in the hatch direction (Fig. 1b). A vent hood was installed approximately 1 m above the reactor. The outlet of the reactor was located on the first floor. After the aging process of approximately 24 h, which was conducted in the reactor, the resulting Ag colloidal suspension was transferred from the reactor to a filtering device through the outlet. The resulting Ag nanoparticles were then filtered and dried in a dryer to remove volatile organic materials and water. Monitoring in the drying room was conducted at site ‘D’ before and after the opening of the dryer door (Fig. 1c). The dried Ag nanoparticles were ground and packaged. In addition, the grinding process was monitored at site ‘G’ where the workers were located. Ventilation facilities near the grinder were installed to prevent the exposure of Ag nanoparticles. The air flow in the grinding room was affected by both the vent hood and the air conditioner. The drying room is separated from the grinding room by a wall and the rooms are connected with a narrow corridor. The distance between the dryer and the grinder is approximately 10 m. All windows in the facility were sealed, to block circulation of the outside wind entering the facility.

Fig. 1 Illustration showing production process flow and measurement locations in a production facility. **a** Production process flow of Ag nanoparticle. Points monitored are *circle* on the left. **b** ‘R’ is the reaction room, c ‘D’ is the drying room, and ‘G’ is the grinding room. Temperature, relative humidity, and air flow at each monitoring site are seen in this figure



Real-time monitoring and sampling

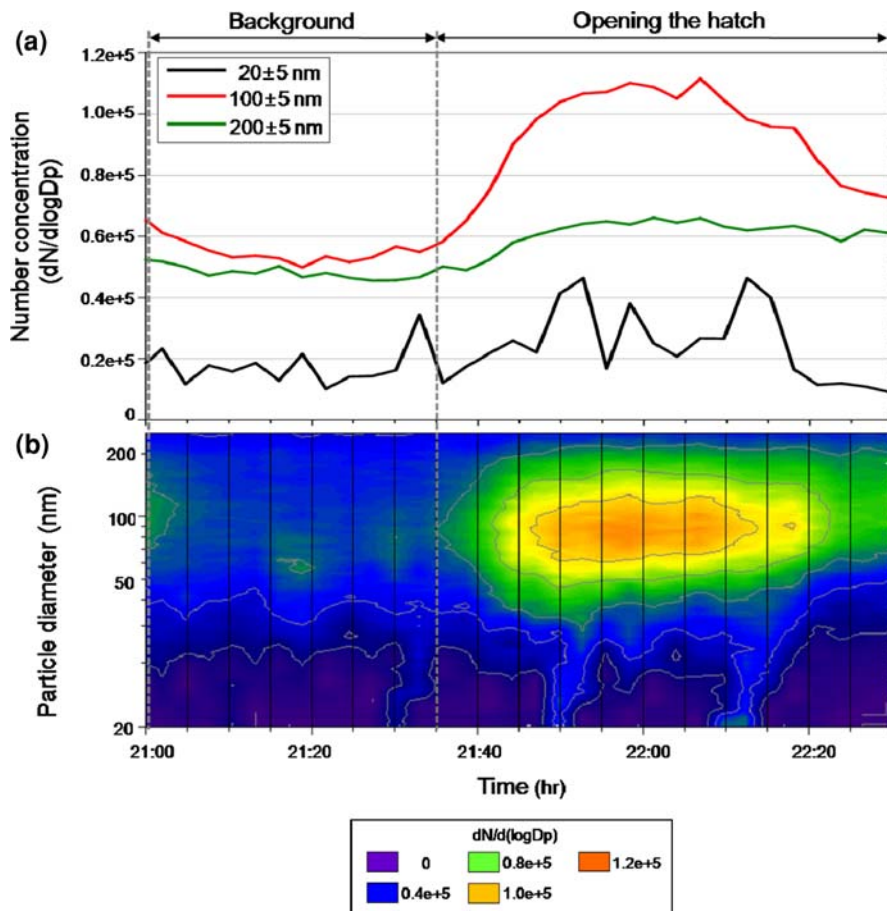
A scanning mobility particle sizer (SMPS) measurement technique is known to be an effective method for measuring nanosize particles in air (Maynard and Kuempel 2005). A SMPS (EPS 4410, CPC 4312, Soft X-ray charger 4530, HCT Co., Korea) equipped with a long differential mobility analyzer (LDMA; DMA 4620, HCT Co., Korea) was used for the real-time measurement of temporal changes in particle size distribution. The LDMA was operated with a sheath flow = 10 L/min and aerosol flow = 1 L/min. An interval between a single scan over the full range of particle sizes required 90 s. The sampling height of SMPS and ESP was 1.2 m. For the analysis of particle morphology, sampling was carried out using an electrostatic precipitator (ESP; Nano Particle Collector 4650, HCT Co., Korea). Particles in air were electrostatically deposited onto a transmission electron microscope (TEM) grid in the precipitator. TEM images of the particles collected during processing were used to confirm the surface area, components, and morphology of the particles.

Results and discussions

Reaction process

The reaction mixture is typically aged for approximately 24 h in the reactor in order to permit the nanoparticles to grow sufficiently. Figure 2 shows the change in particle number concentrations with time during the reaction process. The process for producing Ag nanoparticles began at 8:00 and progressed as described in the experimental section. At 21:35, the reactor hatch was opened for about 1 h for the sampling of Ag nanoparticles. After opening the hatch, the number concentrations of diameter with $100 \pm 5 \text{ nm}$ particles in air rapidly increased when compared to the sizes of $20 \pm 5 \text{ nm}$ and $200 \pm 5 \text{ nm}$ particles as shown in Fig. 2a. This change in concentrations can clearly be seen in the filled contour plot in colors (Fig. 2b). Before opening the hatch, between 21:00 and 21:30, the number of 100 nm particles was approximately $6.1 \times 10^4 \text{ particles/cm}^3$ and the region corresponding to 100 nm are shown in blue and green colors, amounting to 4×10^4 and $6 \times 10^4 \text{ particles/cm}^3$,

Fig. 2 Time series for total particle number concentration measured at site ‘R’ of Fig. 1b during the reaction process between 21:00 to 22:30. **a** Change in the number concentrations of 20 ± 5 , 100 ± 5 , and 200 ± 5 nm diameter particles and **b** change in particle number concentrations between 20 and 250 nm with time is shown as a filled contour plot



respectively. However, the 100 nm particles in air increased after the hatch was opened. The concentration of 100 nm particles at 22:00 was 9.2×10^4 particles/cm³, as indicated by the yellow and red colors, representing 1.0×10^5 and 1.2×10^5 particles/cm³, respectively. Through SMPS results and TEM analyses of samples collected in the reaction process (Fig. 6b, c), it can be concluded that Ag nanoparticles in a solution are aerosolized into the workplace air.

Agglomeration behavior of Ag nanoparticles during the reaction process

Figure 3 shows the change in particle size distribution between 22:00 and 22:30 during the reaction process. A decrease in the number of small particles is clearly seen as the result of the agglomeration of the aerosols. It should be noted that an increase in particle mode diameter was observed with time, as

shown in the inset of the Fig. 3. This suggests that the particles continue to agglomerate in air. Aerosolized particles suspended in air may collide with other particles, because of their relative motion and adherence to form larger particles (Hinds 1999). This relative motion could be the result of Brownian motion, hydrodynamic, electrical, gravitational, or other forces. Agglomeration behavior is also influenced by particle size, mobility, temperature, and concentration. Precise details on the agglomeration of aerosolized particle are beyond the scope of this discussion and have been published elsewhere (Seinfeld and Pandis 1998).

Drying and grinding process

Figure 4 shows measurement data obtained during the drying and grinding process. AgNPs taken from the dryer were cooled for a day at room temperature, and then subjected to grinding. However, measurements

Fig. 3 The change in size distribution of aerosolized particles from 22:01 to 22:26 m after opening the reactor hatch. The *inset* shows the increase in particle mode diameter with time, after fitting by linear regression on the basis of the fit functions

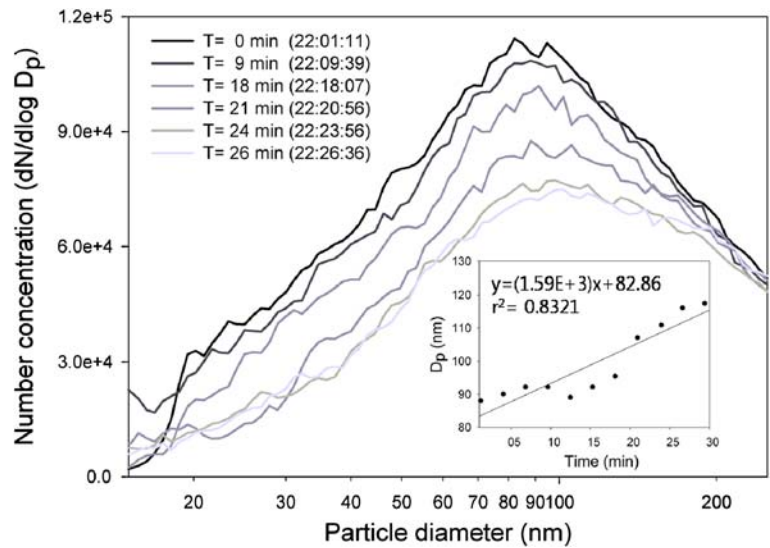
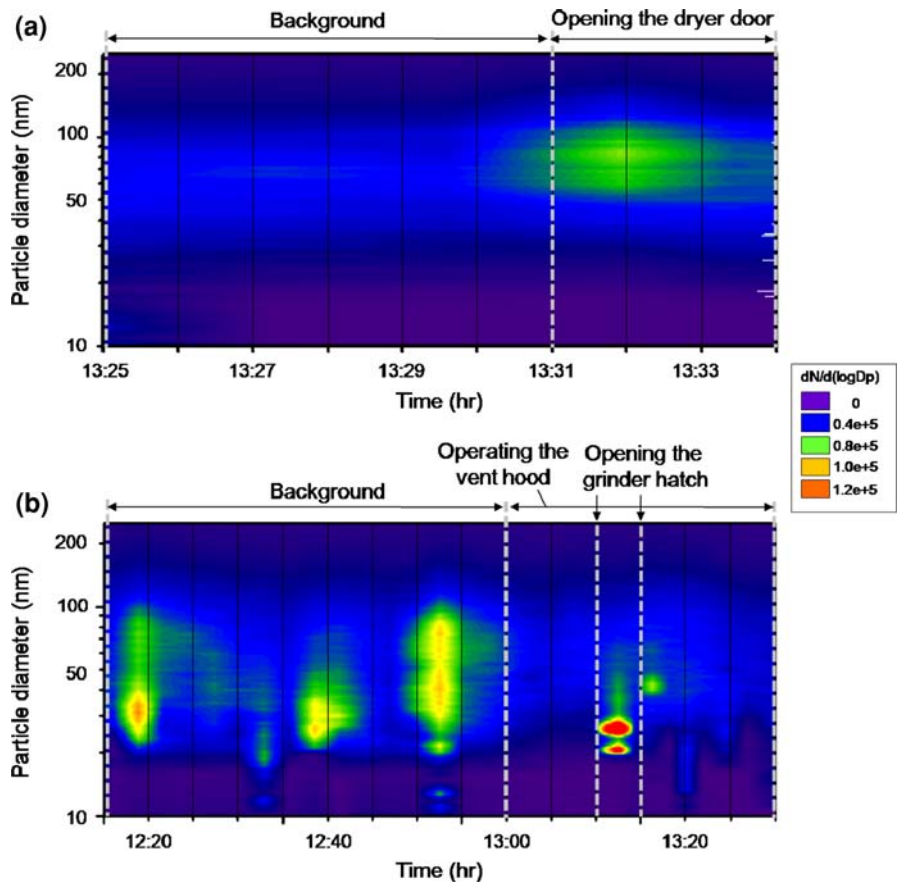


Fig. 4 Time series for total particle number concentrations measured **a** at site ‘D’ of Fig. 1c during the drying process and **b** at site ‘G’ of Fig. 1c during the grinding process



during the grinding and drying process were conducted on the same day. When the dryer door was opened at 13:31, the number of particles in the range of 60–

100 nm was doubled, as seen in Fig. 4a. It should be noted that the SMPS scan required a 90 s interval for a one-point measurement. Therefore, the enhancement

in number concentration from 13:31 to 13:33 can be a momentary phenomenon induced by the temperature and pressure difference inside and outside of the dryer. Figure 4b shows the time series for particle concentration in the case of the grinding room. The grinding process was conducted after lunch time between 12:00 and 13:00. An irregular increase in particle number concentrations was observed because the particles deposited on the floor were scattered by the movements of workers at 12:20, 12:40, and 12:52. The ventilator was switched on at 13:00. After turning on the ventilation system and air conditioner, a reduction in the irregular increase in particle numbers was observed. It is well known that an appropriate ventilation system is useful and effective for reducing exposure to nanomaterials by inhalation (Tsai et al. 2009). When a worker opened the grinder hatch for the packaging of Ag nanoparticles, relatively small sized particles in the range of 30–40 nm were released. This result implies that the grinding process should be conducted in an airtight clean room. In addition, the

ventilation facilities near the grinder are required to protect workers from the exposure to nanoparticles. Importantly, particles deposited on the floor could induce the secondary exposure to nanoparticles.

Comparison of processes

Figure 5 shows a comparison of the size distributions of released particles during the production process. Each peak was calculated after subtracting the background particle concentration. The background was determined as the average number of particles in the same workplace before the start of the operation. The inset of Fig. 5 shows particle size distribution fitted by a lognormal distribution for a clear observation between 20 and 100 nm. The median diameter, geometric standard deviation, and the total number of particles with diameters between 10 and 250 nm, and the change in the total particle concentration during the production process are summarized in Table 1. The highest exposure to Ag nanoparticles in the production

Fig. 5 Measured data on the particle number concentrations during the production process. This result is calculated after the subtraction of particle number concentration of the background. *Inset* is the particle size distribution fitted by a lognormal distribution

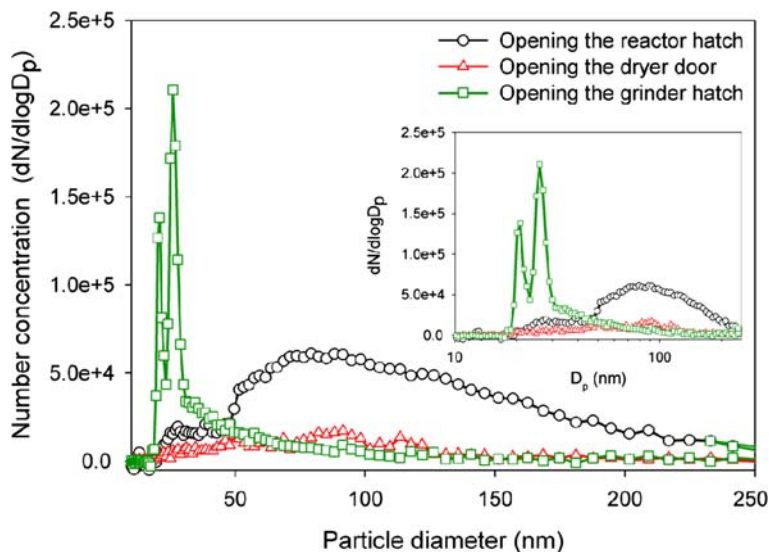
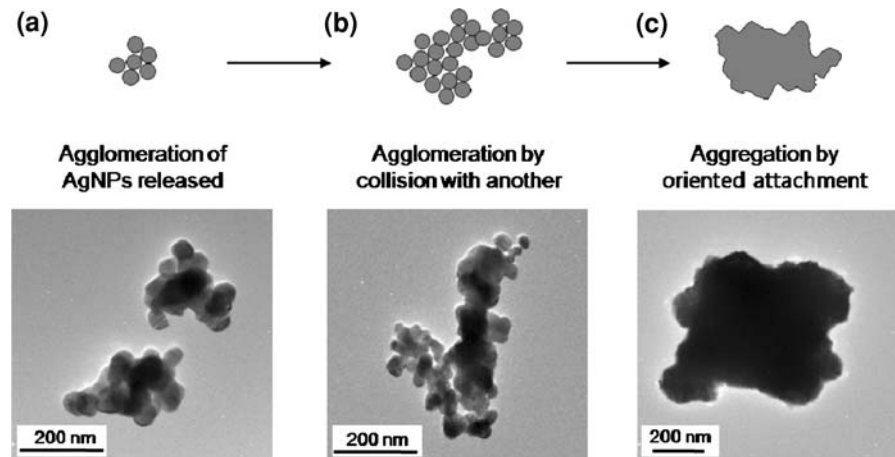


Table 1 Median diameter, geometric standard deviation (GSD), and total number concentration (TNC) with diameters between 10 and 250 nm during the production activity

Location	Activity	Median Dp (nm)	GSD	Total NC (cm ⁻³)	TNC (cm ⁻³)
Reactor	Background	94.75	6.74	7.90e+6	11.02e+6
	Opening the hatch	76.35	4.63	18.92e+6	
Dryer	Background	63.78	6.64	5.11e+6	1.34e+6
	Opening the door	63.78	6.30	6.45e+6	
Grinder	Background	57.25	6.64	4.63e+6	2.45e+6
	Opening the hatch	34.61	6.30	7.08e+6	

Fig. 6 Growth mechanism of aerosolized Ag nanoparticles and TEM images of collected Ag nanoparticles during the product process. **a** and **b** are collected in the reaction room and **c** is collected in the grinding room



process was during the opening the reactor hatch, while the lowest exposure was during the opening of the dryer door. Interestingly, the number of particles released from the liquid phase was larger than that emitted during the handling of dried particles. Small particles released during the grinding process have an increasingly high coefficient of diffusion, leading to increased probability of being deposited in the upper airways. However, if the vapors including nanoparticles evaporated during the reaction process are inhalable, they will lead to the delivery of nanoparticles to the respiratory system (Maynard and Kuempel 2005). Therefore, nanoparticles that are released during the liquid and gas-phase production processes would have different toxicity effects.

Growth mechanism of Ag nanoparticles during the production process

The mechanism by which Ag nanoparticles are aerosolized during the production process can be deduced through the TEM image analysis of Ag nanoparticles collected (Fig. 6). The findings indicate that Ag nanoparticles with diameters of 50–60 nm form agglomerates after the reactor hatch is opened (Fig. 6a). The large surface of the agglomerates and the fast diffusion of small agglomerates in air would induce acceleration in agglomeration. This growth leads to larger agglomerates as shown in Fig. 6b. The degree of agglomeration mainly depends upon the particle mobility and concentration. Particles aggregated with a rough surface were collected during the grinding process, as shown in Fig. 6c. During the dry process, the formation of irregular aggregates at a

relatively low inner temperature (100 °C) of dryer can be explained by growth via oriented attachment. The aggregation of Ag nanoparticles can primarily be attributed to the presence of organic molecules used as dispersing agents. The organic molecules that coat Ag nanoparticles will be replaced by water molecules by the organic ligands that are desorbed during the drying process. The presence of water on the particle surfaces induces oriented attachment, because water molecules enhance Brownian motion and promote growth by bulk diffusion. In addition, a drying time of 24 h is sufficient for the formation of the aggregates at a low temperature (Huang et al. 2003). Additional experimental and theoretical research on the aerosolization mechanism of Ag nanoparticles during the reaction process would be required to obtain a clear, unequivocal explanation of this phenomena.

Conclusion

The exposure characteristics of Ag nanoparticle were monitored and analyzed during a liquid-phase process in a commercial production facility that manufactures nanomaterials. We conclude that Ag nanoparticles are released from the reactor during the liquid-phase production process and agglomerates of Ag nanoparticles are formed in the atmosphere of the workplace. Therefore, the increase in particle number concentration during the liquid-phase process was higher than that during processes that involve the handling of a dry powder. Since risk in liquid-phase process is relatively undervalued compared to the gas or vapor-phase processes, the impact of exposure to

aerosolized nanoparticles in liquid-phase process should be studied in more detail.

Acknowledgments This study was supported by grants (No. 091-071-055) from the Ministry of Environment, Korea. It was also supported by WCU (World Class University) program through the Korea science and Engineering Foundation funded by the Ministry of Education, Science and Technology (400-2008-0230).

References

- Helland A, Scheringer M, Siegrist M, Kastenholz HG, Wiek A, Scholz RW (2008) Risk assessment of engineered nanomaterials: a survey of industrial approaches. *Environ Sci Technol* 42:640–646
- Hinds WC (1999) *Aerosol technology: properties, behavior, and measurement of airborne particles*, 2nd edn. Wiley, New York
- Huang F, Zhang H, Banfield JF (2003) Two-stage crystal-growth kinetics observed during hydrothermal coarsening of nanocrystalline ZnS. *Nano Lett* 3:373–378
- Kreyling WG, Semmler M, Erbe F, Mayer P, Takenaka S, Schulz H, Oberdörster G, Ziesenis AJ (2002) Translocation of ultrafine insoluble iridium particles from lung epithelium to extrapulmonary organs is size dependent but very low. *J Toxicol Environ Health* 65:1513–1530
- Maynard AD, Kuempel ED (2005) Airborne nanostructured particles and occupational health. *J Nanopart Res* 7:587–614
- Oberdörster G, Celein RM, Ferin J, Weiss B (1995) Association of particulate air pollution and acute mortality: involvement of ultrafine particles. *Inhal Toxicol* 7:111–124
- Park J, Kim Y (2008) Effect of shape of silver nanoparticles on the enhancement of surface plasmon resonance (SPR) signals. *J Nanosci Nanotechnol* 8:1–4
- Park J, Lee E, Hwang NM, Kang M, Kim SC, Hwang Y, Park JG, Noh HJ, Kim JY, Park JH, Hyeon T (2005) One-nanometer-scale size-controlled synthesis of monodisperse magnetic iron oxide nanoparticles. *Angew Chem Int Ed* 44:2872–2877
- Schmidt CW (2009) Nanotechnology-related EHS research. *Environ Health Perspect* 117:A158–A161
- Seinfeld JH, Pandis SN (1998) *Atmospheric chemistry and physics*. Wiley, New York
- Tsai SJC, Ada E, Isaacs JA, Ellenbecker MJ (2009) Airborne nanoparticle exposures associated with the manual handling of nanoalumina and nanosilver in fume hoods. *J Nanopart Res* 11:147–161
- Yun HJ, Lee H, Kim ND, Yi J (2008) Characterization of photocatalytic performance of silver deposited TiO₂ nanorods. *Electrochem Commun* 11:363–366